ELSEVIER

Journal of Hazardous Materials 141 (2007) 645–652

Journal of Hazardous Materials

www.elsevier.com/locate/jhazmat

Comparison of dye degradation efficiency using ZnO powders with various size scales

Huihu Wang [a], Changsheng Xie [a,b,*], Wei Zhang [a], Shuizhou Cai [b], Zhihong Yang [a], Yanghai Gui [b]

[a] *State Key Laboratory of Plastic Forming Simulation and Mould Technology, Huazhong University of Science and Technology, Wuhan 430074, PR China*

[b] *Nanomaterials and Smart Sensors Laboratory, Department of Materials Science and Engineering, Huazhong University of Science and Technology, Wuhan 430074, PR China*

Received 9 May 2006; received in revised form 11 July 2006; accepted 11 July 2006
Available online 16 July 2006

Abstract

ZnO powders with various size scales (mean diameter size: 10, 50, 200 and 1000 nm) have been prepared by two different preparation methods, thermal evaporation method and chemical deposition method, and examined as photocatalysts for the UV-induced degradation of methyl orange in water solution. ZnO nanoparticle with diameter size 50 nm prepared by thermal evaporation method showed the highest photocatalytic activity. In addition, the tetrapod ZnO nanopowders had the higher efficiency than irregular ZnO particles. However, the smallest 10 nm ZnO nanoparticle prepared by chemical deposition method indicated the lower efficiency contrast to 200 nm ZnO powders prepared by thermal evaporation method. The results indicated preparation method was the decisive factor rather than size and morphology. Moreover, the effect of catalyst loading, pH value and the initial dye concentration on the final degradation efficiency were discussed through the photocatalytic experiments using 50 nm ZnO nanoparticle as photocatalyst.

Keywords: ZnO nanoparticle; Photocatalytic activity; Size; Morphology; Preparation method

1. Introduction

Excess use of various dyes in the textile industry has led to the severe surface water and groundwater contamination by releasing the toxic and colored effluents, which are usually disposed by various physical and chemical methods, such as coagulation/flocculation [1,2], electrocoagulation [3], coagulation/carbon adsorption process [4] and so on. However, these methods barely transfer the pollutants from one phase to another without destruction or have the other limitations. In recent years, as a promising tool to substitute the traditional wastewater treatment, semiconductor-assisted photocatalysis among the advanced oxide processes (AOP) has attracted the public concern for its ability to convert the pollutants into the harmless substances directly in the waste water. Till now, many kinds of semiconductors have been studied as photocatalysts including TiO_2, ZnO, CdS, WO_3 and so on [5–8]. TiO_2 is the most widely used effective photocatalyst for its high efficiency, photochemical stability, non-toxic nature and low cost. As a contrast, ZnO, a kind of semiconductor that has the similar band gap as TiO_2, is not thoroughly investigated. However, the greatest advantage of ZnO is that it absorbs large fraction of the solar spectrum and more light quanta than TiO_2 [9]. Some researches have highlighted the performance of ZnO on degradation some organic compounds [10,11]. In addition, ZnO has more functions than TiO_2 [12] and recent researches have pointed out that ZnO can also be used in the acidic or alkaline conditions through the proper treatment [13,14]. Therefore, continued study of ZnO is necessary and quite needed.

It is well known the highly reactive $OH^{\bullet}$ radicals and holes is generated on the surface of photocatalyst under the radiation of UV. Therefore, the surface characteristic of ZnO determined by the different fabrication methods will influence this property as well as the final degradation efficiency. The size of pho-

* Corresponding author. Tel.: +86 27 87556544; fax: +86 27 87543776.
E-mail address: csxie@mail.hust.edu.cn (C. Xie).

0304-3894/$ – see front matter © 2006 Elsevier B.V. All rights reserved.
doi:10.1016/j.jhazmat.2006.07.021

tocatalysts is one of the most important factors. There were many comparative studies about the photocatalytic efficiency of pollutants between TiO_2 and ZnO, which emphasized the effectiveness of TiO_2 or ZnO [9,15]. In these studies, Degauss (P-25) TiO_2 (mean diameter, 25 nm) and commercial ZnO (mean diameter, 200 nm) are the most commonly used effective photocatalysts. However, the problem is the great size discrepancy of the two different kinds of photocatalysts. Besides that, the photocatalytic properties of colloidal ZnO nanoparticle with diameter size in a range from 5 to 15 nm prepared by chemical deposition method are also discussed widely [16,17]. Nevertheless, the researches about the photocatalytic property of ZnO photocatalysts with diameter size 30–60 nm and micron size are still remained limitedly, especially the ZnO nanoparticles prepared by thermal evaporation that have a higher photoactivity. In order to compare the photocatalytic property of ZnO with that of TiO_2 roundly, the research about the photocatalytic property of ZnO with different size scales is significative. Except for size, morphology and fabrication methods of the photocatalysts are the other crucial factors that influence the degradation efficiency severely [18]. Demonstrating the relationship between the surface characteristics of photocatalysts and the photocatalytic activities of ZnO is beneficial to the development of catalysts and can be of use in preparing photocatalysts with high activity.

In this study, various ZnO powders with different size ranging from 10 nm to micron grades were compared for the photodegradation efficiency of methyl orange aqueous solution. The influences of size, morphology and preparation method on the photocatalytic property of ZnO powders prepared by evaporation–condensation method and chemical deposition method were studied. For the ZnO powders with diameter size 50 nm, the experiments were conducted to investigate the effects of different experimental conditions on the final photodegradation efficiency.

2. Experimental procedure

2.1. Synthesis of ZnO powders with various size scales

ZnO powders with four kinds of size scales, including 10, 50, 200 and 1000 nm, were obtained. Therein, 200 nm commercial ZnO powders prepared by thermal evaporation method were purchased. One part of commercial ZnO powder was used as photocatalyst without further treatment. The other part of commercial ZnO powder was used as raw materials to prepare the 1000 nm ZnO powders by agglomerating in sintering furnace at 800 °C for 8 h. The synthesis procedures of 10 and 50 nm ZnO powders were described in detail as following.

The chemical precipitation method was used to prepare 10 nm ZnO colloidal nanoparticle. The reagents used in the preparation process were purchased from Shanghai Chemicals Co. Ltd. with analytic grade. In the 500-mL conical flask, 11.0 g zinc acetate hydrate ($Zn(Ac)_2{\cdot}2H_2O$, with 99.9% purity) were dissolved in 500 mL ethanol solvents. Then, 2.9 g lithium hydroxide monohydrate was added into the solution. Through ultrosonicating, a transparent solution was obtained. After that, the conical flask was put into the water tank with a constant temperature 60 °C and 10 ml distilled water was added into the conical flask. To fabricate ZnO colloidal nanoparticle, the as-prepared solution was agitated by a magnetron for 30 min at 60 °C. The 10 nm ZnO powders were collected from the solution by centrifuge and dried at 60 °C without washed.

Two kinds of 50 nm ZnO powder, pure tetrapod and irregular nanoparticle, were prepared by evaporation–condensation method. The experimental setup used for evaporation–condensation was self-designed and described in the literature elsewhere [19,20]. In this experiment, a graphite crucible containing the small Zn ingot was put into the chamber of the experimental set-up and heated only by the high-frequency induction thermal resource. The chamber was pumped to the low vacuum state and sequentially filled with a mixed $Ar + O_2$ gas to 1.0×10^4 Pa. In the preparation process, the oxygen partial was controlled at 0.6×10^3 Pa by adjusting the gas flux ratio of $Ar:O_2$. The different ZnO powders were collected from the different parts of water-cooled wall of the chamber.

2.2. Characterization of ZnO powders

Size and morphology of the 10 nm no-washed ZnO nanoparticle were recorded by transmission electron microscopy (TEM) with Tecnai G2 20 microscope using an accelerating voltage 200 kV. The other ZnO powders were observed by Sirion 200 field emission scanning electron microscopy (FESEM). The crystal structure identification of 10 nm ZnO was obtained using Philips X'pert X-ray diffractormeter with Cu $K\alpha_1$ radiation in the 2θ range from 20° to 80°. FT-IR spectrums of 10 nm ZnO were identified with a VERTEX 70 Spectrometer. The BET surface areas and the pore volumes of different ZnO powders were obtained by using ASAP 2020 instrument.

2.3. Photocatalytic experiment of different ZnO powders

By measuring the photodegradation efficiency of methyl orange with a definite concentration in aqueous solution under the illumination of UV, the photocatalytic activity of different ZnO powders were evaluated reliably. All the experiments were done at temperature 27 ± 2 °C. Two UV lamps (Philips) that predominantly emit at 254 nm with the definite power 15 W were employed as the light source and positioned parallel to the 500 mL Pyrex glass bottle that was used to load the dye solutions in the photocatalytic process. The distance between the top of Pyrex glass bottle and the UV lamp was 10 cm and the light intensity was about 4.0×10^3 μW/cm^2. The photocatalytic experiments were carried out with 200 mL methyl orange solutions, which were sonicated for 15 min and stirred in the dark for 20 min after the addition of photocatalysts. The molecular structure of methyl orange is shown in Scheme 1. Four milliliters samples were performed at intervals of 15 min in two

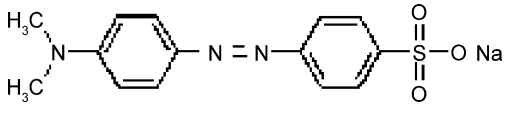

Scheme 1. The molecular structure of methyl orange.

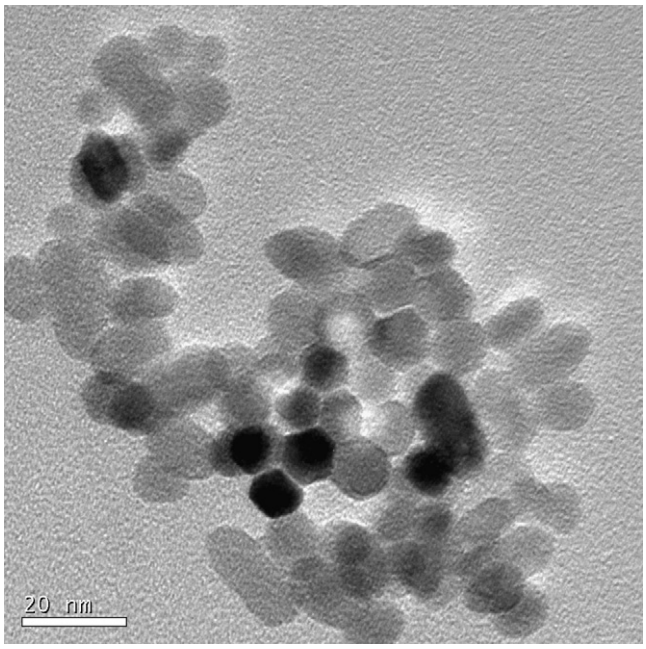

Fig. 1. TEM image of ZnO nanoparticle prepared by chemical deposition method.

continuous hours. For investigating the effects of pH values on the photodegradation efficiency, 1 mol/L NaOH and HCl solution were used to adjust the pH values of the pure dye solutions before the photocatalysts were added.

The photodegradation efficiency was monitored by measuring the absorbance of the solution samples at its maximum absorption wavelength of 464 nm with UV–vis spectroscopy. The decolorization efficiency as a function of time was calculated by the absorbency values of the original and analytical samples.

3. Results and discussion

3.1. Powder characterization

The morphology and size of obtained ZnO powders were characterized by TEM and FESEM. Fig. 1 shows the transmission electron micrograph of the original ZnO colloidal nanoparticle prepared by chemical deposition method. It can be observed that ZnO nanoparticle mainly presents rod and hexangular shape with mean diameter 10 nm. The XRD pattern of the prepared 10 nm ZnO powders is shown in Fig. 2. All the diffraction peaks can be indexed as the hexagonal wurtzite ZnO with lattice constants in agreement with the values in the standard card (JCPDS 36-1451). No other diffraction peaks are detected. Moreover, the particle size calculated by Deby–Scherrer equation from the XRD result is about 9 nm, which is accordant with the TEM result.

The pure terapod ZnO powders and main irregular ZnO nanoparticle were obtained from evaporation–condensation method by collecting the products in the different parts of water-cooled wall, which are shown in Fig. 3a and b, respectively. The mean diameter of the irregular ZnO nanoparticle is about 50 nm,

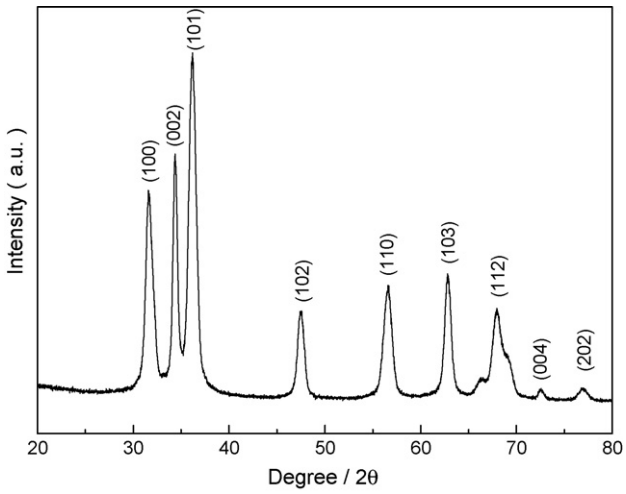

Fig. 2. XRD pattern of ZnO nanoparticle prepared by chemical deposition method.

which is much smaller than the powders prepared by chemical deposition method.

The commercial ZnO powder and its calcined samples at 800 °C are given in Fig. 3c and d, respectively. No obvious change in morphology was observed when the commercial ZnO powders were sintered for 8 h at 800 °C. Both ZnO powders present irregular shape. However, the size of calcined samples increases from the original 200 nm of commercial ZnO powders to above 1000 nm.

The BET surface areas and pore volumes of different ZnO powders were shown in Table 1. It can be seen that the BET surface area increases with the increase of particle size. The 10 nm ZnO prepared by chemical bath deposition has the largest surface area (49.24 m^2/g)and the 1000 nm ZnO powders calcined at 800 °C has the lowest surface area(0.71 m^2/g).

3.2. Evaluation of the photocatalytic activity

3.2.1. Comparison of catalytic activities of ZnO powders

All the ZnO powders were selected for the evaluation of the photocatalytic activity under the illumination of UV light. In order to study the effect of the light on the degradation of methyl orange, blank experiment was performed under UV light without the addition of photocatalysts, which verified that methyl orange of 20 mg/L was photolyzed only up to 2% in 2 h. This degradation efficiency was negligible when the different photocatalysts were added into the solution. When there was no UV light, the concentration of methyl orange with the addition of

Table 1
BET surface areas and pore volumes of different ZnO particles

Sample	BET surface area (m^2/g)	Pore volume (cm^3/g)
10 nm ZnO nanoparticles	49.24	0.04
50 nm ZnO nanoparticles	9.35	0.017
Tetrapod ZnO nanoparticles	12.65	0.018
200 nm ZnO particles	2.28	0.008
1000 nm ZnO particles	0.71	0.002

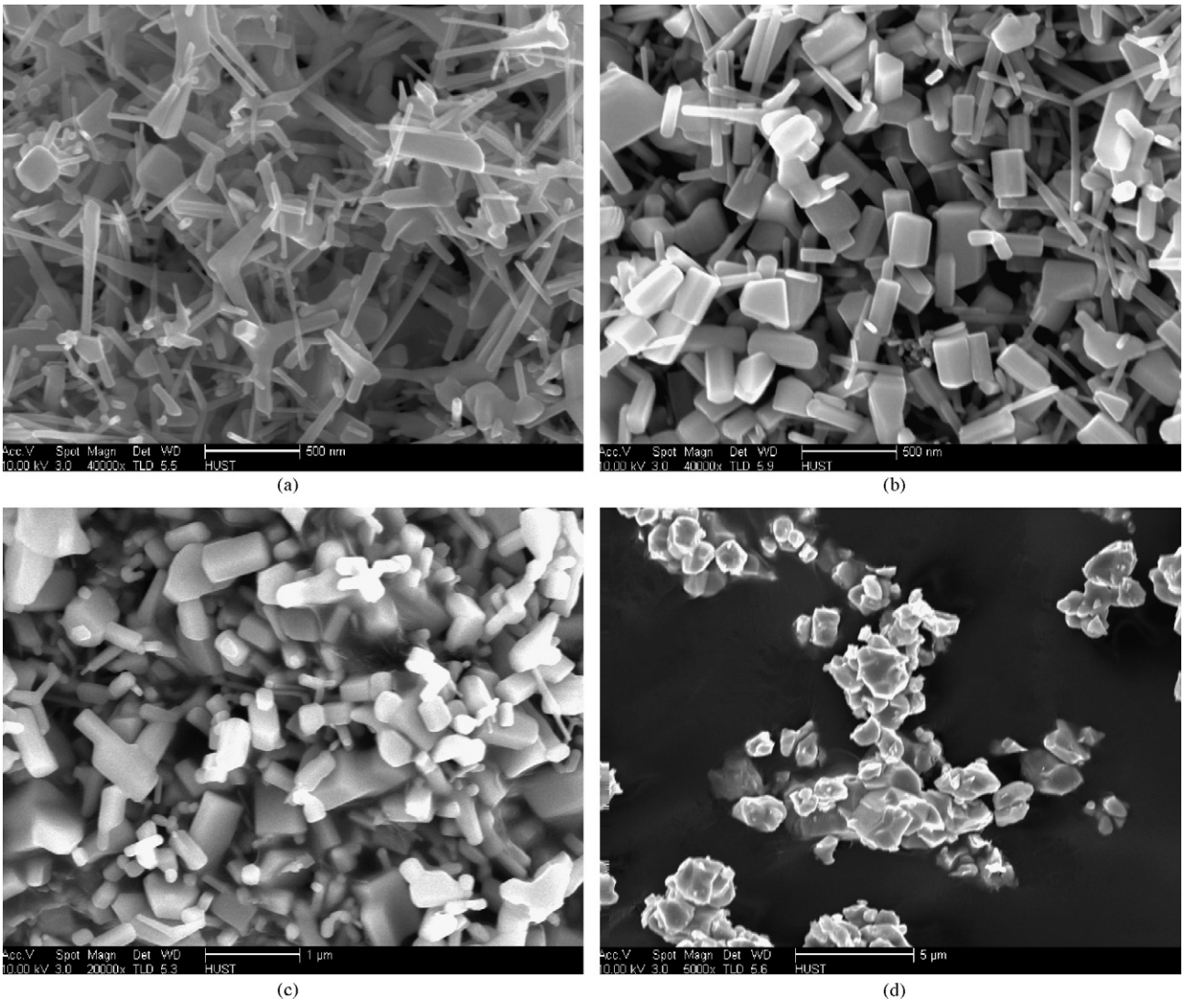

Fig. 3. FESEM images of ZnO powders prepared by thermal evaporation method: (a) tetrapod ZnO powders; (b) 50 nm ZnO particles; (c) commercial ZnO particles; (d) micron ZnO particles.

ZnO photocatalysts kept stable in 2 h. From the blank experiments, it can be concluded that UV light and photocatalysts are the necessary factors in the photocatalytic process.

Fig. 4 shows the photodegradation results of various ZnO powders at dye concentration = 20 mg/L, catalyst loading = 0.3 g/L, reaction time = 2 h, initial pH value = 6. It was found that the addition of catalysts enhanced the degradation efficiency to a different degree in contrast to the blank experiment. Furthermore, the typical results of Fig. 4 gave us the intuitionistic impression about the effect of size on the degradation efficiency for the four different ZnO catalysts with various size scales, including nanometer, submicron, and micron grade. For ZnO catalysts prepared by thermal evaporation method, it can be observed the decolorization efficiency after illuminated 2 h reduced in the order nanometer > submicron > micron grade, which is given in the a–c curve respectively. Additionally, the difference in degradation efficiency between nanometer grade and submicron grade is quite larger than the one between submicron and micron grade, indicating the possible jump of ZnO

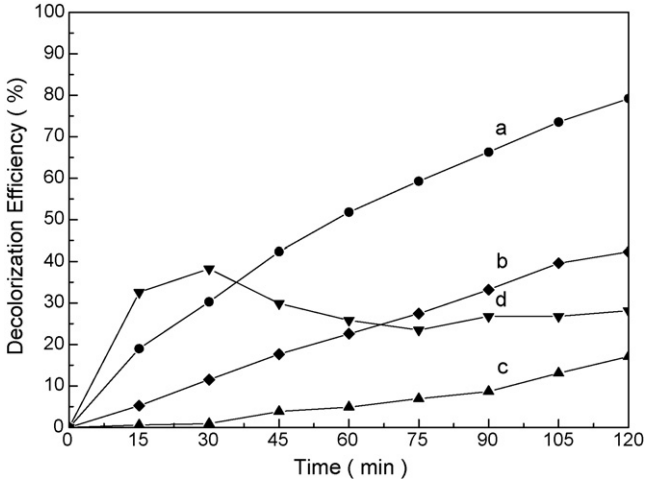

Fig. 4. Decolorization efficiency vs. time for different ZnO particles: (a) 50 nm ZnO particles; (b) 200 nm commercial ZnO particles; (c) micron ZnO particles; (d) 10 nm ZnO particles.

activity from submicron into nanometer grade. However, for the photocatalytic activity of ZnO nanoparticle prepared by different fabrication methods, the size is not the most important factor, which can be seen from the Fig. 4d curve that expresses the degradation efficiency of ZnO nanoparticle with the mean diameter size 10 nm. In the initial 15 min illuminated by UV lights, the degradation efficiency of dye is the largest among the four ZnO powders. However, the final degradation result of ZnO powders with diameter 10 nm after 2 h illumination is even lower than ZnO powders with diameter 200 nm. Moreover, unlike the stable photocatalytic activity of ZnO powders prepared by thermal evaporation method, this kind of ZnO nanoparticle shows the inherent instability on photodegradation process, which is suggested by the undulation of the curve (Fig. 4d) and the small change of degradation efficiency after 15 min, indicating the insignificant size effect and the greater influence of preparation method.

The effect of size on the photodegradation efficiency can be ascribed to three reasons: when the size of ZnO particles decreases, (1) the amount of the dispersion particles per volume in the solution will increase, resulting the enhancement of the photon absorbance; (2) at the same time, the surface area of ZnO photocatalyst will increase, which will promote the adsorption of more dye molecules on the surface; (3) furthermore, the simple couple of photoexcited electron–hole pairs will be suppressed. Then the photocatalytic activity of ZnO powders prepared by thermal evaporation method is in the order as followed: nanometer > submicron > micron grade. For the decreased photocatalytic activity of ZnO nanoparticle with diameter 10 nm, it indicated that the preparation method is a crucial factor though the size was the smallest among the four ZnO powders. To discover the inherent factor, the surface characteristics of ZnO powders were detected by FT-IR technique, which was given in Fig. 5. The spectrum of ZnO nanoparticle with diameter 10 nm has the absorption broad bands at about 1415 and 1584 cm^{-1}, corresponding to C–O, C=O stretching in acetate groups, which verify the coverage state of ZnO colloidal nanoparticle. The small absorption band at 1341 cm^{-1} is

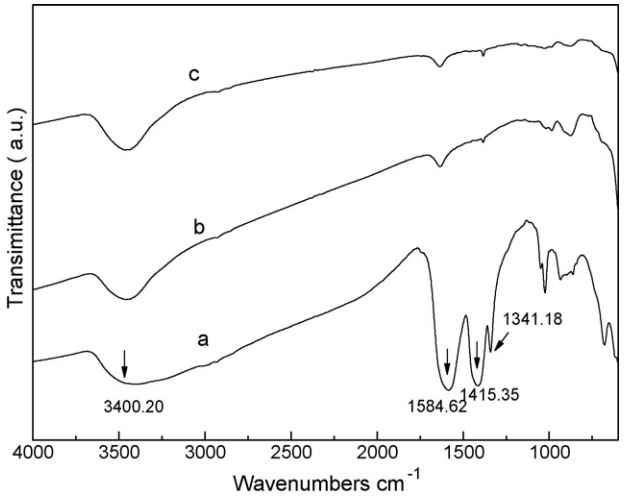

Fig. 5. FTIR spectrums of three kinds of ZnO photocatalysts: (a) 10 nm ZnO particles; (b) 50 nm ZnO particles; (c) commercial ZnO particles.

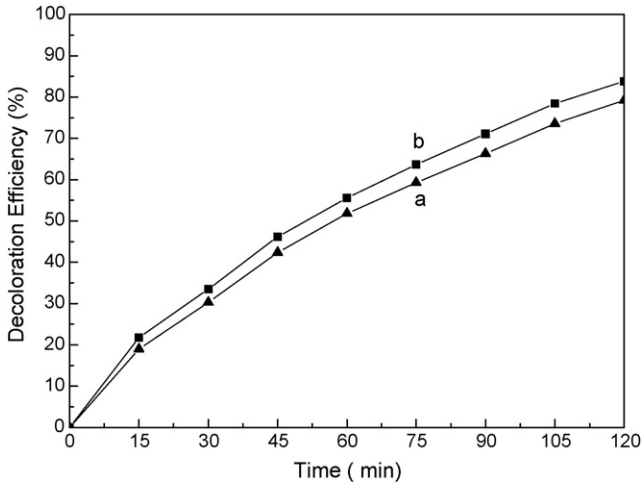

Fig. 6. Photodegradation efficiency of methyl orange with (a) 50 nm ZnO particles; (b) tetrapod ZnO powders.

probably due to the weakly bound acetic acid molecules, which does not chemisorb to the surface of nanoparticle (as shown in Fig. 5a). However, the spectrum of ZnO powders prepared by thermal evaporation has only one bigger absorption band at 3400 cm^{-1} corresponding to the vibration of the hydroxyl, which is similar to 10 nm ZnO nanoparticle. The FT-IR results indicated clearly that the fabrication method rather than size was the most important factor that determined the photocatalytic activity of ZnO. The more photocatalytic behavior of 10 nm ZnO nanoparticle will be introduced in the other paper.

In Fig. 6, the effect of morphology on the photodegradation efficiency is reported in the 20 mg/L methyl orange solution with 0.3 g/L photocatalysts at the fixed reaction time (2 h) and pH value. The percentage of decolorization efficiency is evaluated. For the tetrapod ZnO powders, it has the higher efficiency than ZnO particles up to 5% in 2 h. This can be ascribed to the unique three-dimensional branched morphology, which resisted the aggregation of ZnO powders in the solution. In addition, the surface planes of tetrapod ZnO powders would also benefit the photodegradation process. However, the effect of morphology on the photocatalytic efficiency is the lowest contrast to that of the fabrication method and the size. Studies performed with different ZnO powders that presented different morphologies indicated that crystallinity played the key role rather than particle size for the same preparation method and morphology was in the highest flight for the different preparation method [18]. In this study, for the performances of different ZnO powders, it can be seen the fabrication method is the decisive factor and the particle size, morphology are the secondary factors.

3.2.2. *Catalytic activity of 50 nm ZnO nanoparticles*

Except for the effect of catalyst type, the different experimental conditions are also the crucial factors that determine the final photodegradation efficiency. For little reports have been studied on the photocatalytic performances of 50 nm ZnO powders prepared by thermal evaporation method, the subsequent experiments were carried out with this kind of ZnO nanoparticle.

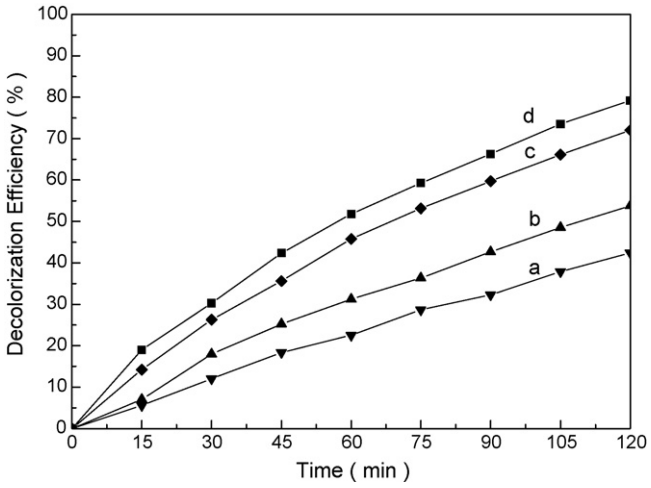

Fig. 7. Effect of catalyst concentration on the photodegration efficiency: (a) 0.05 g/L; (b) 0.1 g/L; (c) 0.2 g/L; (d) 0.3 g/L.

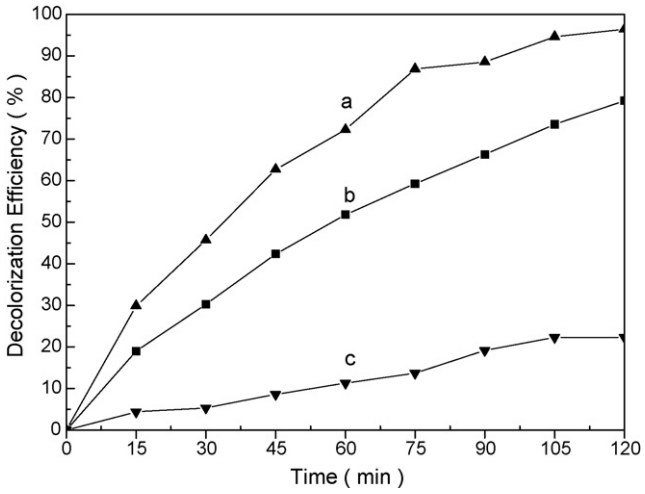

Fig. 8. Effect of initial dye concentration on the photodegradation efficiency: (a) 10 mg/L; (b) 20 mg/L; (c) 30 mg/L.

3.2.2.1. Effect of catalyst concentration. To investigate the effect of catalyst loading on the final decolorization efficiency, a series of experiments were carried out by varying the catalyst from 0.05 to 0.3 g/L in the solution with 20 mg/L dye concentration. The rate of degradation is illustrated in Fig. 7. It is demonstrated that the decolorization efficiency is increasing with the catalyst-loading enhancement. However, the increase of final efficiency after 2 h illumination is not well proportioned with the multiple increase of catalyst. Many other researches have been verified that there was an optimum amount of catalyst loading under different experimental conditions [21]. When the catalyst concentration is below this optimal value, it is assumed that the photocatalytic degradation is determined by the effective surface of catalyst and the adsorption of UV light. At lower catalyst loading, the adsorption of light controls the photocatalytic process due to the limited catalyst surface. Whereas, the possible aggregation of catalyst is also the limiting factors as well as the light scattering. In this study, with the multiple increase of catalyst, the surface that adsorbs the photon is not increasing in a geometrical ratio for the inclination to aggregation. Moreover, there is a decrease in UV light penetration as a result of light scattering effect with an increase of the turbidity of the suspension, leading to the reduction of the effective photoactivated volume of suspension. The integration of these two reasons results in the small increase of decolorization efficiency rather than the linearly increase with the multiple increase of catalyst loading.

3.2.2.2. Effect of initial dye concentration. Fig. 8 demonstrates the effect of initial dye concentration on the rate of decolorization efficiency by varying the initial concentration from 10 to 30 mg/L with the constant ZnO catalyst loading (0.3 g/L) and pH values. The results reveal that the initial dye concentration influences the degradation efficiency severely. With the increase of initial dye concentration, the degradation efficiency decreases remarkably, especially when the initial dye concentration varies from 20 to 30 mg/L. The negative effects of the initial dye concentration are ascribed to the competence between dye and OH^- ion adsorption on the surface of catalyst. The adsorption of dye depresses the OH^- ion adsorption, which results in the reduction on the formation of hydroxyl radicals. At the same time, as the initial dye concentration increases, the path length of photons entering the solution decreases. Hence in the solution with constant catalyst concentration, the formation of hydroxyl radicals that can attack the pollutants decreases, thus leading to the lower decolorization efficiency.

3.2.2.3. Effect of pH values. The effect of pH values on the degradation efficiency is studied in the pH range 3–12 at the dye concentration = 0.3 g/L and initial dye concentration = 20 mg/L. Fig. 9 demonstrates the results of decolorization efficiency after 2 h illumination in the solution with different pH values. It can be seen a fast increase in the degradation of methyl orange with increase of the pH value from 3 up to 10 followed by the abruptly decrease at pH 12. As an amphoteric oxide, ZnO can be dissolved both at acidic and alkaline environment. Evgenidou et al. has measured the zinc ion to verify that the low initial reaction rates at acidic pH are attributed to dissolution and photodissolution of ZnO. In this work, at the lower pH value (pH 3), since the

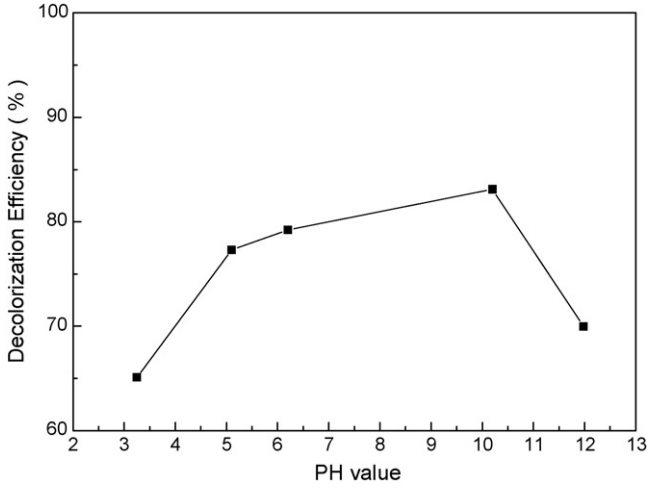

Fig. 9. Effect of pH value on the photodegradation efficiency.

dissolution of ZnO, the effective catalysts is reduced greatly, which induces the depressing of photodegradation process [22].

In the pH range 5–10, the surface characteristic of ZnO nanoparticle is the limiting factor for pH values can change its surface charge property. It has been reported that the pH of zero-point charge for ZnO is 9.0 [23]. When pH value is higher than 9 (pH 10), the ZnO surfaces is negatively charged by adsorbing OH^- ions, which favors the formation of hydroxyl radicals. However, when pH value is lower than 9, the ZnO surface is preferentially covered by the dye molecules. Therefore, with the increase of pH value, the higher pH can provide higher OH^- ions to form more hydroxyl radicals, consequently enhancing the photodegradation efficiency. On the other hand, with the increase of pH value, the electrostatic repulsion between the MO anion and the oxide surface gradually increases [24]. In that case, the slow diffusion of surface-generated $OH^\bullet$ towards the double layer to the low concentration of methyl orange anion will make the photodegradation process of methyl orange slower than direct charge transfer [25]. For the competition of the two factors, the highest decolorization efficiency was obtained at pH 10. However, at pH 12, the decolorization efficiency decreased greatly.

4. Conclusions

ZnO powders differing in the size and morphology were prepared by two different preparation methods and exploited their photocatalytic activities in degradation of methyl orange dye. It was found that the size of ZnO powders prepared by thermal evaporation method played the key role in the photocatalytic performance through contrastively studying the degradation efficiency of 50, 200, and 1000 nm ZnO photocatalysts. At the same time, morphology was also a potential factor that influenced the final degradation efficiency by demonstrating the photocatalytic performance of tetrapod and irregular ZnO nanoparticle. However, the photocatalytic efficiency of ZnO nanoparticle with diameter 10 nm prepared by chemical deposition method was even lower than that of 200 nm ZnO powders prepared by thermal evaporation method, which revealed the decisive role of preparation method contrast to the size and morphology of ZnO powders.

The experiments were conducted with 50 nm ZnO powders to investigate its photocatalytic activity under various process conditions. The results indicated that the catalyst loading, pH values and the initial dye concentration affected the degradation efficiency of ZnO powders obviously. We learned that the photodegradation efficiency is enhanced with the increase of catalyst loading and the reverse effect is obtained with the increase of initial dye concentration in our experiments. The photocatalytic decomposition of methyl orange was most efficient in the solution at pH 10.

Acknowledgements

We thank the financial support by National Natural Science Foundation of China (NSFC, Grant Nos. 50271029, 50041024).

References

[1] C. Allegre, M. Maisseu, F. Charbit, P. Moulin, Coagulation–flocculation–decantation of dye house effluents: concentrated effluents, J. Hazard. Mater. B 116 (2004) 57–64.
[2] V. Golob, A. Vinder, M. Simonic, Efficiency of the coagulation/flocculation method for the treatment of dyebath effluents, Dyes Pigm. 67 (2005) 93–97.
[3] A. Alinsafi, M. Khemis, M.N. Pons, J.P. Leclerc, A. Yaacoubi, A. Benhammou, A. Nejmeddine, Electro-coagulation of reactive textile dyes and textile wastewater, Chem. Eng. Process. 44 (2005) 461–470.
[4] S. Papic, N. Koprivanac, A. LoncaricBozic, A. Metes, Removal of some reactive dyes from synthetic wastewater by combined Al(III) coagulation/carbon adsorption process, Dyes Pigm. 62 (2004) 291–298.
[5] B. Liu, T. Torimoto, H. Yoneyama, Photocatalytic reduction of CO_2 using surface-modified CdS photocatalysts in organic solvents, J. Photochem. Photobiol. A: Chem. 113 (1998) 93–97.
[6] I. Konstantinou, T. Sakellarides, V. Sakkas, T. Albanis, Photocatalytic degradation of selected *S*-Triazine herbicides and organophosphorus insecticides over aqueous TiO_2 suspensions, Environ. Sci. Technol. 35 (2001) 398–405.
[7] Y.T. Kwon, K.Y. Song, W.I. Lee, G.J. Choi, Y.R. Do, Photocatalytic behavior of WO_3-loaded TiO_2 in an oxidation reaction, J. Catal. 191 (2000) 192–199.
[8] H. Lin, S. Liao, S. Hung, The dc thermal plasma synthesis of ZnO nanoparticles for visible-light photocatalyst, J. Photochem. Photobiol. A: Chem. 174 (2005) 82–87.
[9] S. Sakthivel, B. Neppolian, M.V. Shankar, B. Arabindoo, M. Palanichamy, V. Murugesan, Solar photocatalytic degradation of azo dye: comparison of photocatalytic efficiency of ZnO and TiO_2, Sol. Energy Mater. Sol. C 77 (2003) 65–82.
[10] C.A.K. Gouvea, F. Wypych, S.G. Moraes, N. Duran, N. Nagata, P. Peralta-Zamora, Semiconductor-assisted photocatalytic degradation of reactive dyes in aqueous solution, Chemosphere 40 (2000) 433–440.
[11] C. Lizama, J. Freer, J. Baeza, H.D. Mansilla, Optimized photodegradation of Reactive Blue 19 on TiO_2 and ZnO suspensions, Catal. Today 76 (2002) 235–246.
[12] P.V. Kamat, R. Huehn, R. Nicolaescu, A "sense and shoot" approach for photocatalytic degradation of organic contaminants in water, J. Phys. Chem. B 106 (2002) 788–794.
[13] R. Comparelli, E. Fanizza, M.L. Curri, P.D. Cozzoli, G. Mascolo, A. Agostiano, UV-induced photocatalytic degradation of azo dyes by organic-capped ZnO nanocrystals immobilized onto substrates, Appl. Catal. B: Environ. 62 (2005) 144–149.
[14] O.A. Fouad, A.A. Ismail, Z.I. Zaki, R.M. Mohamed, Zinc oxide thin films prepared by thermal evaporation deposition and its photocatalytic activity, Appl. Catal. B: Environ. 62 (2006) 144–149.
[15] E. Evgenidou, K. Fytianos, I. Poulios, Semiconductor-sensitized photodegradation of dichlorvos in water using TiO_2 and ZnO as catalysts, Appl. Catal. B: Environ. 59 (2005) 81–89.
[16] S.B. Park, Y.C. Kang, Photocatalytic activity of nanometer size ZnO particles prepared by spray pyrolysis, J. Aerosol. Sci. 28 (1997) 3473–3474.
[17] M.L. Curri, R. Comparelli, P.D. Cozzoli, G. Mascolo, A. Agostiano, Colloidal oxide nanoparticles for the photocatalytic degradation of organic dye, Mater. Sci. Eng. C 23 (2003) 285–289.
[18] D. Li, H. Haneda, Morphologies of zinc oxide particles and their effects on photocatalysis, Chemosphere 51 (2003) 129–137.
[19] R. Wu, C. Xie, H. Xia, J. Hu, A. Wang, The thermal physical formation of ZnO nanoparticles and their morphology, J. Cryst. Growth. 217 (2000) 274–280.
[20] D.W. Zeng, B.L. Zhu, C.S. Xie, W.L. Song, A.H. Wang, Oxygen partial pressure effect on synthesis and characteristics of Sb_2O_3 nanoparticles, Mater. Sci. Eng. A. 366 (2004) 332–337.
[21] A. Akyol, H.C. Yatmaz, M. Bayramoglu, Photocatalytic decolorization of Remazol Red RR in aqueous ZnO suspensions, Appl. Catal. B: Environ. 54 (2004) 19–24.

[22] E. Evgenidou, K. Fytianos, I. Poulios, Photocatalytic oxidation of dimethoate in aqueous solutions, J. Photochem. Photobiol. A: Chem. 175 (2005) 29–38.

[23] G.A. Parks, The isoelectric points of solid oxides, solid hydroxides, and aqueous hydroxo complex systems, Chem. Rev. 65 (1965) 177–198.

[24] C. Wang, J. Zhao, X. Wang, B. Mai, G. Sheng, P. Peng, J. Fu, Preparation, characterization and photocatalytic activity of nano-sized ZnO/SnO_2 coupled photocatalysts, Appl. Catal. B: Environ. 39 (2002) 269–279.

[25] I. Poulios, M. Kositzi, A. Kouras, Photocatalytic decomposition of triclopyr over aqueous semiconductor suspensions, J. Photochem. Photobiol. A: Chem. 115 (1998) 175–183.